ACS OMEGA

http://pubs.acs.org/journal/acsodf

Article

Nanonization of Magnoflorine-Encapsulated Novel Chitosan–Collagen Nanocapsules for Neurodegenerative Diseases: *In Vitro* Evaluation

Dar Junaid Bashir, Saliha Manzoor, Imran A. Khan, Masarat Bashir, Nidhi Bharal Agarwal, Shweta Rastogi, Indu Arora,* and Mohammed Samim*

Cite This: *ACS Omega* 2022, 7, 6472–6480

Read Online

ACCESS | Metrics & More | Article Recommendations

ABSTRACT: Neurodegeneration is one of the most common diseases in the aged population, characterized by the loss in the function of neuronal cells and their ultimate death. One of the common features in the progression of this type of diseases is the oxidative stress. Drugs which are currently being used have been found to show lateral side effects, which is partly due to their inefficiency to cross blood–brain barrier. Nanoencapsulation of bioactive compounds is a profound approach in this direction and has become a method of choice nowadays. This study involved the evaluation of the anti-oxidative properties of magnoflorine (MF), which is an aporphine quaternary alkaloid, and synthesis of MF-loaded chitosan–collagen nanocapsules (MF-CCNc) for its better efficacy as a potent anti-oxidant. Physiochemical characterization of the synthesized nanocapsules was done by using dynamic light scattering and transmission electron microscopy. It revealed that the synthesized nanocapsules are of small size range, as small as 12 ± 2 nm, and are more or less of spherical shape. Sustained release was shown by MF in the *in vitro* drug release studies. Both MF and MF-CCNc were found to have good anti-oxidant potential with IC_{50} < 25 μg/mL. No major cytotoxicity was shown by the synthesized nanocapsules on SH-SY5Y cells. *In silico* anti-acetylcholinesterase (AChE) studies were also done, and they revealed that MF can be a potent inhibitor of AChE.

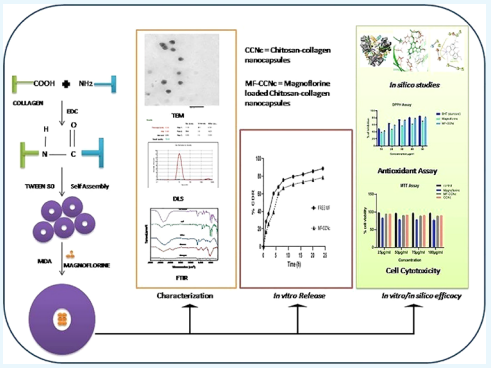

1. INTRODUCTION

Neurodegenerative diseases which are characterized by loss in the neuronal activity, due to the neuronal cell death, have potentially affected the human population in the recent past.[1,2] Alzheimer's disease (AD) and Parkinson's disease (PD) are two of the most common neurodegenerative diseases of the modern era. AD in particular had posed a serious threat in the recent times, according to an estimate made by Alzheimer's Association in its 2015 report; a threefold increase is expected in people living with dementia worldwide from 46.8 million now to 131.5 million in 2050, while its 2019 report shows 123% increase in the number of deaths due to AD from 2000 to 2015 and it is quite alarming. The disease is characterized by impaired levels of acetylcholinesterase (AChE), formation of β-amyloid plaques and neurofibrillary tangles in the brain at the molecular level, and loss of memory and cognitive deficit at the behavioral level.[3,4] Oxidative stress and hence the mitochondrial dysfunction are believed to play an important role in the proliferation of Alzheimer's, Parkinson's, Huntington's, and other neurodegenerative diseases.[5−8] Treatment is still illusive, and the focus is still on the AChE inhibitors in AD and dopamine agonists in PD with most of the drugs in the market belonging to these groups.[9−11] As of now, scientists have explored many other pathways for drug administration that limit the use of currently available medications.

Plant alkaloids due to their structural diversity have been used as therapeutics for different brain disorders. Galantamine and rivastagmine are the two alkaloids which are currently used for the treatment of patients suffering from AD. Besides these two alkaloids, caffeine, indomethacin, huperzine A, berberine, and indirubin have also shown efficacy against AD to some extent.[12] In the current study, we have chosen magnoflorine (MF) which is also an alkaloid. MF is an aporphine alkaloid and possesses antioxidant and antiradical properties.[13] It exerts an inhibitory effect against Cu^{2+}-induced lipid peroxidation of high density lipoprotein which is beneficial for lipid metabolism.[14] It has also shown cognition and antiamnestic

Received: August 17, 2021
Accepted: February 7, 2022
Published: February 16, 2022

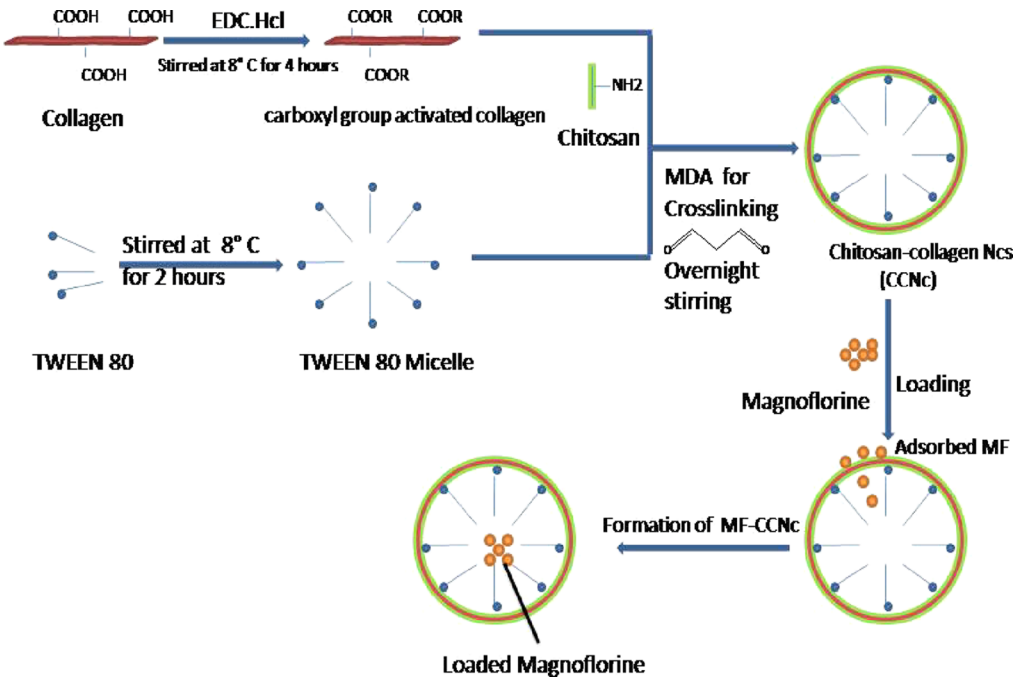

Figure 1. Schematic representation of preparation of MF-loaded chitosan−collagen nanocapsules.

properties in the passive avoidance (Pa) test.[15] MF due to its antioxidant and antiradical properties can reduce the oxidative stress and hence mitochondrial dysfunction in AD, PD, and other neurodegenerative diseases.

The use of current therapeutics for neurodegenerative diseases is limited by the blood−brain barrier (BBB); nanoparticles due to their ability to cross BBB easily have proven to be more effective.[16,17] To avoid the hindrance from the BBB, nanoparticle-mediated drug delivery to the brain has been used and it has shown a lot of promise.[18,19] Dual functional nanoparticles have shown better efficacy against AD and other neurodegenerative diseases, as they get easily absorbed by the gastrointestinal tract, can cross the BBB more easily, and avoid cytotoxicity to a much larger extent.[20−22] These things led to the development of nanotechnology-based therapeutics, which gained popularity as nanomedicine and is becoming a method of choice specially for neurodegenerative diseases.[23,24] Chitosan, a polysaccharide, and collagen, a protein, are two biomaterials which are widely being used as drug delivery vehicles for neurodegenerative diseases.[25,26] With the introduction of protein−polysaccharide drug delivery vehicles, focus has shifted to chitosan−collagen nanocomposites as well, as their scaffolds have shown tremendous promise.[27−29] Substantial efforts are being made for alternate therapy which involves nanoformulations of the active principle of some medicinal plants, especially alkaloid molecules which will lead to the better efficacy for neurodegenerative diseases.

In this context, the present work is focused on the evaluation of anti-oxidant property of MF to take the advantage of the nanoparticle strategy for the preparation of a novel drug delivery system in order to increase the efficacy of MF against oxidative stress and to further enhance its delivery to the brain with less cytotoxicity. *In silico* AChE property of MF was also evaluated.

2. MATERIALS AND METHODS

2.1. Chemicals and Reagents. Chemicals procured from Sigma-Aldrich [chitosan, malondialdehyde (MDA), dimethylsulfoxide (DMSO), MF, and acetylcholinesterase (AChE) from electric eel (type-VI-S)], chemicals procured from Spectrochem [1-(3-dimethylaminopropyl)-3-ethyl carbodiimide-hydrochloride (EDC·HCL)], chemicals procured from SD Fine [Tween 80], chemicals procured from Thermo Fisher Scientific Inc. [Dulbecco's modified Eagle medium (DMEM), 10% fetal bovine serum (FBS), and (3-(4,5-dimethythiazol-2-yl)-2,5-diphenyltetrazolium bromide) (MTT)], and chemicals procured from Himedia Laboratories [5,5′-dithiobis(2-nitrobenzoic)acid (DTNB) and acetylthiocholine iodide (ATCl)] were used.

2.2. Preparation of Chitosan−Collagen Nanocapsules. Briefly, 10% of chitosan and 10% of collagen solutions were prepared separately in 10 mL of double-distilled water each. 1 mL of this collagen solution was added to 10 mL of double distilled water, and it was left for stirring. After 30 min of stirring, 1 mg of EDC·HCL was added to this solution and it was left for 1 h for stirring. To this solution, 1 mL of chitosan solution was added and it was left for 16 h for stirring. 1 mL of the abovementioned solution was added to a solution, which was prepared simultaneously by adding 150 μL of Tween 80 in three lots of 50 μL each (addition after every 15 min) to 10 mL of double-distilled water in a round bottom flask and was allowed to stir for 8 h. 0.5 mg of MDA was added to this solution, and it was left for further stirring overnight. The solution was then dialyzed for 48 h using spectropore membrane dialysis bag (12 kDa cut-off), and water was exchanged after every 4 h (Figure 1).

2.3. Characterization. *2.3.1. Drug Loading.* 2 mg of MF was dissolved in 3 mL of DMSO for the preparation of a solution of MF in DMSO. This was then slowly added to 2 mL (1 mg/mL of nanocapsules in double-distilled water) of chitosan−collagen nanocapsular solution separately with continuous vortexing to obtain MF-loaded nanocapsules.

https://doi.org/10.1021/acsomega.1c04459
ACS Omega 2022, 7, 6472−6480

These drug-loaded nanocapsules were then dialyzed for 24 h using a dialysis bag of 12 kDa molecular weight cut-off; water was changed after every 4 h to remove excess DMSO.

2.3.2. Physicochemical Characterization. To analyze the chemical interactions in the formation of nanocapsules, Fourier-transform infrared spectroscopy (FTIR) was used. FTIR was recorded from 4000 to 400 cm^{-1} using a Bruker Alpha instrument. For the determination of average particle size and size distribution, determination dynamic light scattering (DLS) was done. Zetasizer Nano ZS (Malvern Instruments Corp., Malvern, UK), Jamia Hamdard, was used for DLS measurements. For the determination of the shape and size of nanocapsules, transmission electron microscopy (TEM) analysis was done. A HR-TEM (JEOL JEM-1400) instrument at Indian Institute of Technology Delhi, India was used for TEM analysis.

2.3.3. Encapsulation Efficiency and In Vitro Release Study. Encapsulation efficiency gives us the percentage of drugs which have gone inside the nanocapsules relative to the total amount of drugs which were added to the solution. To determine the percentage EE of MF-loaded chitosan−collagen nanocapsule (MF-CCNc) solution, the nanocapsular solution was centrifuged (15 000 rpm for 1 h at 4 °C).[30] The supernatant was collected, filtered, and used for determination of untrapped MF from the solution using a UV spectrophotometer at 329 nm. The encapsulation efficiency (EE) for the MF was calculated as follows:

$$EE = [(MF_{total} - MF_{free})/MF_{total}] \times 100\%$$

where MF is the active principle (MF), MF_{total} is the total amount of active principle which was loaded, and MF_{free} is the amount of free MF present in the solution.

For *in vitro* release studies, the dialysis bag method (dialysis bag, 12−14 kDa cut-off value) was used.[31] 1 mL of MF solution and 1 mL of loaded NCs (containing 0.5 mg of MF each) were placed in two separate dialysis bags. These samples were then placed in 20 mL phosphate buffer (pH 7.4) and stirred at 50 rpm and room temperature. At different time "*t*" intervals (1, 2, 4, 6, 8, 12, 16, 20, and 24 h), 2 mL of the sample was withdrawn and replaced with 2 mL of fresh phosphate buffer. The samples were then analyzed using a UV spectrophotometer at 329 nm. To determine cumulative percentage of released MF, the concentration of MF at different time "*t*" intervals was calculated using the straight line equation, that is, $y = bx + c$, where "*y*" is the absorbance at time "*t*", "*x*" is the concentration at time "*t*", and *b* and *c* are slope and intercept, respectively. As 2 mL of the sample was withdrawn from 20 mL dissolution medium and filled with 2 mL of fresh PBS calculate at different time intervals, the following equation was used to calculate the % CDR:

$$\%\,CDR = \frac{C_n V + V_i \sum_{i=0}^{n=i} C_i}{A_{MF}} \times 100\%$$

where % CDR is the cumulative amount of MF released, *V* (mL) is the total dissolution volume, and C_n (mg/mL) and V_i (mL) are the concentration and volume at "*n*" and "*i*" time point, respectively. A_{MF} is the initial amount of MF (mg) present in the samples.

The release data so obtained were fitted into different mathematical models: zero order, first order, Higuchi, Korsmeyer−Peppas, and Hixson−Crowell.[32]

2.3.4. Cytotoxicity Studies. Cytotoxicity studies were done using human neuroblastoma cell line, SH-SY5Y cells. These were grown in DMEM media, with 10% heat inactivated FBS at 37 °C; the incubator was provided with 5% CO_2. Cells were also cultured timely in the same media. To see the effect of MF-CCNc *versus* MF alone and nanocapsules without MF at different concentrations on SH-SY5Y cells, 2×10^5 SH-SY5Y cells were seeded in 16-well plates (4 wells for each concentration) with DMEM that were supplemented with 10% FBS in 5% CO_2 incubator. Four experiments were carried out in triplicate ($n = 12$), and increased concentrations of MF, MF-CCNC, and CCNc were given for 24 h; one well which was neither given MF, MF-CCNC, nor CCNc was considered as control. MTT assay was used to determine the cell viability, and reading was taken by the ELISA plate reader at 590 nm.[33,34] The equation mentioned below was used to calculate the percentage of cell viability:

$$\%\,viability = (A_t/A_c) \times 100\%$$

where A_t is the absorbance obtained for the tested formulations and A_c is the absorbance obtained for the control.

2.3.5. Free Radical Scavenging Assay (Antioxidant Assay). To determine the antioxidant potential of MF and MF-CCNc, a standard method was used.[35] Briefly, 1 mL of DPPH (0.1 mM) in methanol was added to different concentrations (10, 20, 30, 40, and 50 μg/mL) of MF and MF-CCNc. The mixture was first shaken vigorously using vortex, and then it was allowed to stand in the dark for 4 h, after which the absorbance was taken at 517 nm with a UV−visible spectrophotometer. Butylated hydroxytoluene (BHT) (10, 20, 30, 40, and 50 μg/mL) was used as the standard, and the scavenging activity was calculated as follows:

$$\text{scavenging activity} = \frac{A_{standard} - A_{test\ sample}}{A_{standard}} \times 100\%$$

where $A_{standard}$ and $A_{test\ sample}$ are the absorbances of the standard and the test sample, respectively.

2.3.6. In Silico Studies. Schrodinger 2016 was used for docking studies, while the ligand was optimized using the DFT-631g basis set in Jaguar. The protein was downloaded from RCSB.org using PDB: 1EVE and E2020. With the help of Glide package, it was then constructed to perform the protein preparation wizard.[36] To avoid the unnecessary interactions, water molecules were removed. The LigPrep module was used in the preparation of ligands for docking.[37] The preparation of protein was done using optimized potential liquid simulation (OPLS-2005) force field and *N*-acetate and *N*-methyl as capping residues. The active site was predicted using the Sitemap module, where site I was the site reported in the crystal structure. Thus, site I was used to perform docking, as it was the site reported in the crystal structure of the standard ligand. The prepared ligand was used for developing the conformers using the instructed stereochemistry intact, and IFD studies were done.

2.3.7. Acetylcholinesterase Inhibition Assay. The modified Ellman method was used to determine the anti-acetylcholinesterase (AChE) activities of MF and MF-loaded nanocapsules.[38,39] Briefly, AChE (10 μL at 10 U/mL) in 50 mM Tris-HCL buffer (pH 8.0/7.4) solution with various concentrations (10−50 μg/mL) of MF, MF-CCNc, and CCNc alone was incubated for 45 min at room temperature in a 96-well cell culture plate. 125 μL of 3 mM DTNB was

https://doi.org/10.1021/acsomega.1c04459
ACS Omega 2022, 7, 6472−6480

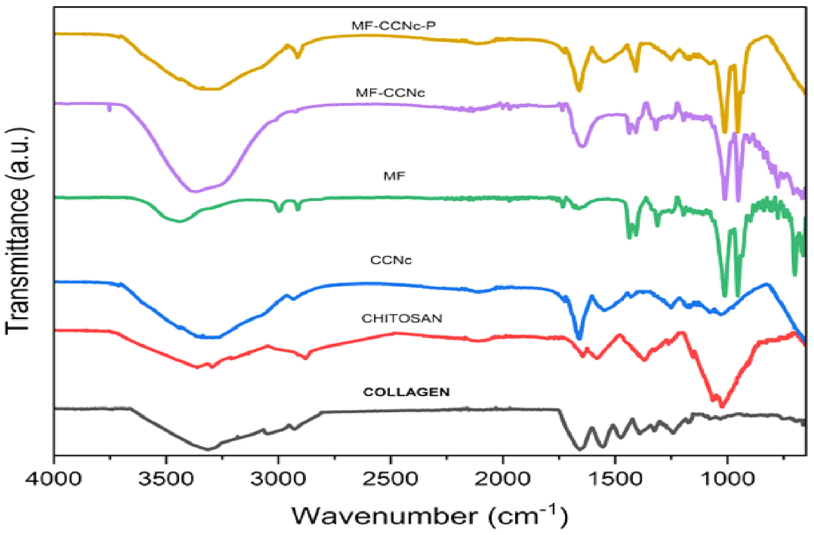

Figure 2. FTIR spectrum of collagen, chitosan, chi−col nanocapsules, MF, MF-CCNc, and MF-CCNc-P.

added after the incubation of reaction mixture, and total volume was made upto 300 μL with 50 mM Tris-HCL buffer (pH 8.0/7.4). 50 μL of 15 mM ATCl was added to initiate the enzyme activity. The hydrolysis of ATCl was assessed at 405 nm using a UV−visible spectrophotometer. 10−50 μg/mL of anti-acetylcholinesterase drug donepezil was used as positive control. The percentage of inhibition of AChE was determined using the formula

2.4. Statistical Analysis. The data from individual groups were presented as the mean ± standard deviation (SD). All the statistical analyses were performed on GraphPad Prism v8 (GraphPad Software, San Diego, CA, United States) and Origin 2020b. Statistical analysis of variance between treated and control groups was done using one-way ANOVA and Duncan's multiple range tests in GraphPad Prism v8.4. The minimum criterion for statistical significance was set at $p < 0.05$ for all the comparisons.

3. RESULTS AND DISCUSSION

3.1. FTIR Analysis. Figure 2 shows the FTIR spectrum of collagen, chitosan, chitosan−collagen nanocapsules {CCNc}, MF, and MF-CCNc. The characteristic peaks of collagen are observed in Figure 2. A strong Peak at 1658 cm^{-1} corresponding to C═O stretching vibrations of amide I is evident besides peaks at 1554 and 1235 cm^{-1} corresponding to N−H bending and C−N stretching, respectively.[40] The characteristic peaks of chitosan are observed in Figure 2. FTIR of chitosan (b) has shown all the characteristic peaks of chitosan. A broad peak at 3620−3282 cm^{-1} which corresponds to N−H, O−H stretching, and intermolecular hydrogen bonding is visible. Weak peaks at around 3368 and 3288 cm^{-1} of N−H of free amine are also found on this broad peak. A sharp peak at around 1647 cm^{-1} which corresponds to C═O of the residual *N*-acetyl group and peaks at 1589 and 1325 cm^{-1} for N−H bending of the primary amine and C−N stretching of amide III are also confirmed. Prominent peaks at 1066 and 1028 cm^{-1} for C−O stretching are also confirmed.[41] The FTIR spectrum of CCNc shows a broad peak at 3631−3210 cm^{-1} corresponding to N−H, O−H and intermolecular hydrogen bonding. Weak peaks of free amine, which were confirmed in chitosan at 3360 and 3294 cm^{-1} were absent in this region. It is due to the interaction of free amine with collagen, leading to the formation of new amide bonds. Peaks at 1176, 1076, and 1030 cm^{-1} correspond to C−O−C bridging and C−O, as reported for chitosan−collagen scaffolds by Rezaii *et al.* due to the interactions at the molecular level.[42] A sharp peak at 1655 cm^{-1} corresponds to C═O of amide; it is of high intensity due to the formation of new amide bonds. Collagen also has this amide C═O peak at around 1658 cm^{-1}; however, it is broader and of low intensity. The peak corresponding to free amine which was evident in chitosan was absent in CCNc, as free amine of chitosan has interacted with collagen which has led to the formation of chitosan−collagen nanocapsules. However, a medium peak at 1554 cm^{-1} corresponding to N−H bending of amide II was evident. The FTIR spectrum of MF shows a medium less broad peak around 3450−3620 cm^{-1} corresponding to the free −OH group of MF. Medium peaks at 3002 and 2905 cm^{-1} correspond to the C−H stretching of alkene and alkane, respectively. Medium and multiple peaks from 1550 to 1400 cm^{-1} corresponding to aromatic C═C stretch are also apparent. A sharp peak at 1021 cm^{-1} corresponding to C−O stretch is also evident. The FTIR spectrum of MF-CCNc shows a broad peak from 3580 to 3250 cm^{-1} corresponding to the intermolecular hydrogen bonding of −OH of MF with CCNc. A more or less sharp peak at 1650 cm^{-1} corresponding to the C═O of amide of CCNc is also prominent. Medium and multiple peaks from 1550 to 1400 cm^{-1} corresponding to aromatic C═C stretch of MF besides a sharp peak corresponding to C−O stretch 1021 cm^{-1} are also apparent, which confirms the formations of MF-CCNc. The FTIR spectrum of the physical mix of MF and chitosan−collagen nanocapsules MF-CCNc-P showed major peaks of both MF and CCNc without much change in the frequency and intensity, indicating that there is less physical interaction. Extensive hydrogen bonding interactions are evident in the case of MF-CCNc in comparison to MF-CCNc-P. A high intensity broad peak at 3550−3620 cm^{-1} corresponds to it; further, a medium peak at 1554 cm^{-1} corresponding to N−H bending which is evident in MF-CCNc-P has shifted toward the C═O peak and merged into it, leading to its broadening due to this extensive hydrogen bonding.

3.2. DLS and HR-TEM Analysis. Size analysis of the MF-loaded nanocapsules was done by using DLS and TEM. DLS for MF-CCNc showed a hydrodynamic diameter of 10.59 nm

https://doi.org/10.1021/acsomega.1c04459
ACS Omega 2022, 7, 6472−6480

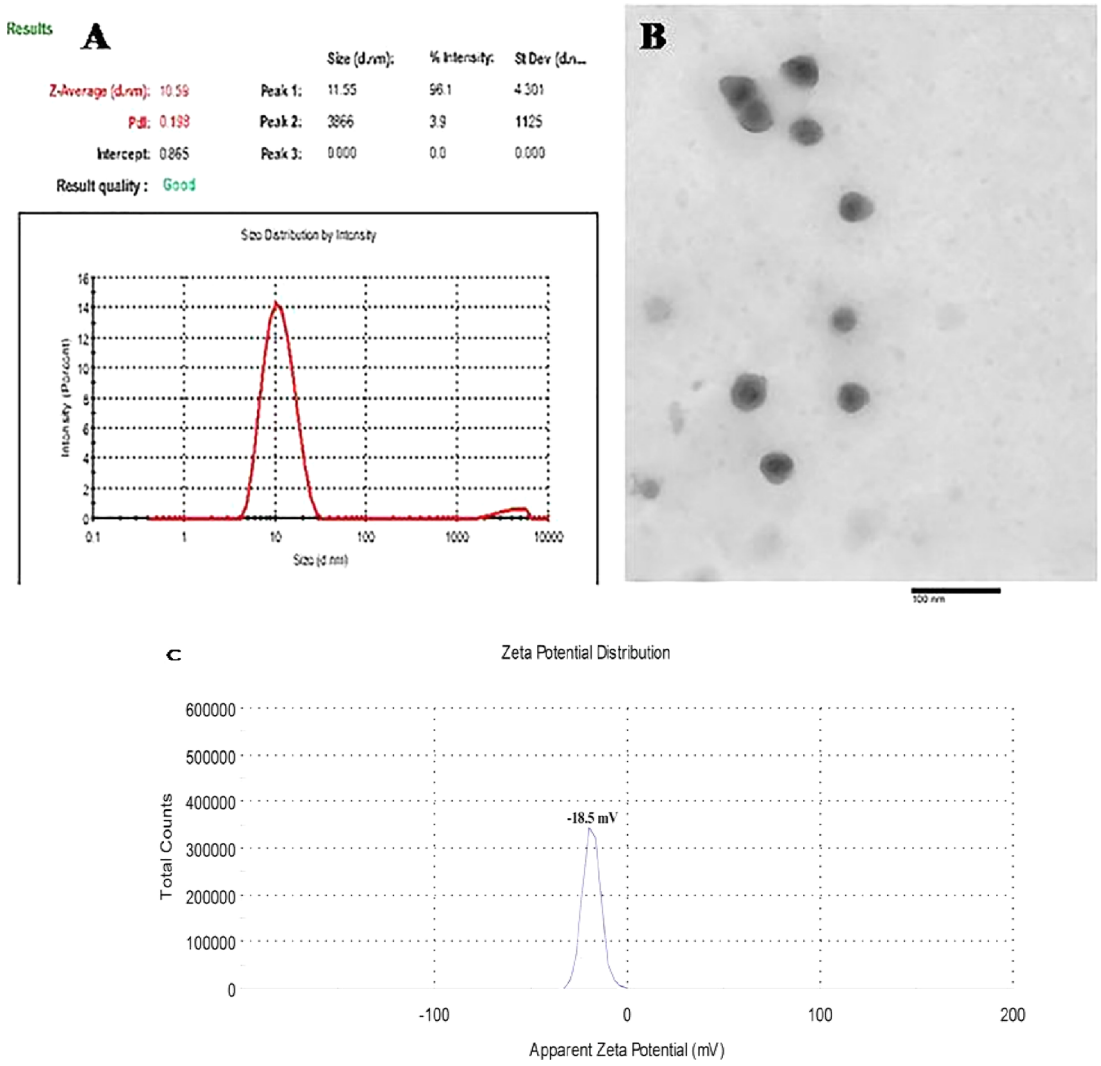

Figure 3. (A) DLS, (B) TEM, and (C) ζ potential results of MF-loaded chitosan−collagen capsules.

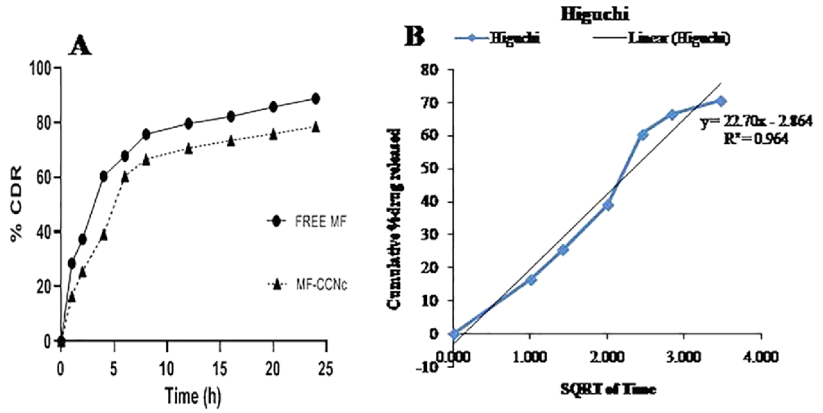

Figure 4. (A) % CDR, that is, cumulative drug release and hence *in vitro* release kinetics of MF from nanocapsules. (B) Best fitted model for the released nanocapsules.

and a polydispersity index (PDI) of 0.198 (Figure 3A). A similar size of 12 ± 2 nm with spherical morphology was found in the TEM image (Figure 3B). ζ potential of the synthesized nanocapsules was found to be −18.5 ± 2 mV (Figure 3C), indicating that the nanocapsules are quite stable. Usually, the ζ potential from +30 to −30 mV is considered stable in the suspended state.[43]

3.3. Encapsulation Efficiency and *in Vitro* Release Study. Encapsulation efficiency of MF-CCNc was found to be 76 ± 1%. Cumulative percentage of MF released from MF-CCNc in PBS (pH 7.4) was plotted as a function of time, as shown in Figure 4A.

The release studies of MF-CCNc have shown biphasic behavior. Within the first 4 h itself, an initial burst release was

https://doi.org/10.1021/acsomega.1c04459
ACS Omega 2022, 7, 6472−6480

observed, which was followed by a sustained release till 24 h of study similar to the pattern which have been observed by the most nanodrug delivery systems.[44] MF (60.41 ± 2%) was released in the first 4 h and (88.76 ± 1.4%) was released in 24 h. MF-CCNc has shown a slower release rate than MF, (39.12 ± 1.5%) of MF-CCNc was released in first 4 h, while 78.53 ± 1% was released after 24 h of the study. Burst release of MF in comparison to MF-CCNc can be attributed to free −OH in MF. The release data so obtained were fitted into different models, and Higuchi was found as the best fit model with a value of 0.964, as shown in Figure 4B. The Higuchi model implies that the amount of MF liberated from the MF-CCNc is a function of square root of time. The fact that MF-CCNc follows the Higuchi model implies that the drug release pattern is more or less through diffusion, as the significance of this model is that it is more applicable for the diffusion mechanism unlike other models.[45]

3.4. Cytotoxicity Studies. To determine the cellular response for MF, MF-CCNc, and CCNc, cell viability was determined using MTT assay. The human neuroblastoma SH-SY5Y cell line was used in this study. Four different concentrations (6.25, 12.5, 25, and 50 μg/mL) of the test samples were used for the studies. The cell viability (%) of MF, MF-CCNc, and CCNc was determined after their incubation with SH-SY5Y cells for 24 h in a MTT assay. The results as depicted in Figure 5 clearly indicate that cell viability is in the

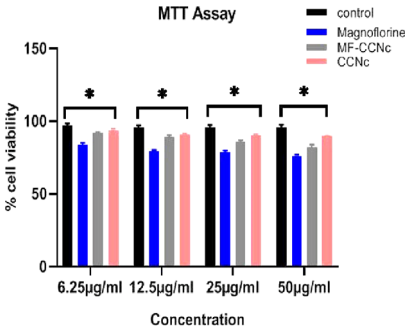

Figure 5. Cell viability assay results of MF, MF-CCNc, and chitosan−collagen nanocapsules at different concentrations. Asterisk (*) over a line denotes statistically significant ($p < 0.05$) value of control with MF, MF-CCNc, and CCNc. Values are expressed as mean ± SD ($n = 3$).

order CCNc > MF-CCNc > MF. At the maximum concentration of 50 μg/mL, cell viability of CCNc, MF-CCNc, and MF is 93.25, 85.50, and 79.45%, respectively, at ($p < 0.05$). From the results, it can be concluded that there were no major cytotoxic effects at the used concentrations and the nanocapsules further help in lowering the cytotoxicity of the active principle to some extent.

3.5. Antioxidant Assessment of MF and MF-CCNc. Oxidative stress is one of the main characteristics of neurodegenerative diseases, which is found in the disease pathology of diseases like Parkinson's and Alzheimer's.[46] DPPH radical scavenging assay was used to evaluate the anti-oxidant potential of MF and MF-CCNc. The results (Figure 6) showed that both MF and MF-CCNc possess significant ($p < 0.05$) DPPH scavenging activity ($IC_{50} < 25$ μg/mL). At the maximum concentration, that is, 50 μg/mL, the inhibition values are 69 ± 1.61 and 81 ± 1.42%, respectively, for MF and MF-CCNc, which was compared to standard anti-

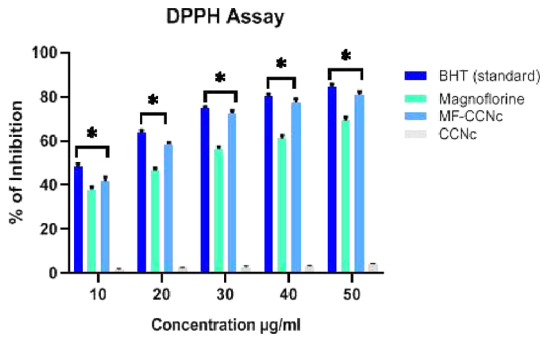

Figure 6. Free radical scavenging ability of BHT (standard), MF, and MF-loaded chitosan and collagen nanocapsules. Asterisk (*) over a line denotes statistically significant ($p < 0.05$) value of control with MF, MF-CCNc, and CCNc. Values are expressed as mean ± SD ($n = 3$).

oxidant BHT (84 ± 1.32%). Anti-oxidants help in diminishing and delaying the progression of diseases like Alzheimer's, Parkinson's, and other diseases. From the abovementioned study, it was evaluated that both MF and MF-CCNc can act as good anti-oxidants; it was further evaluated from the results that MF-CCNc had got higher anti-oxidant activity in comparison to MF. This may be primarily because of the presence of chitosan, which itself acts as an anti-oxidant.

3.6. *In Silico* Study. Docking studies showed that there are three similar sites on the protein, and site-1 was used (Figure 7A). MF showed interaction at site-1 (Figure 7B−D).The SP and XP scores were obtained better for the MF than the standard ligand (Aricept), as it has the least rotatable bond (=0) in comparison to standard (=24) offering Erotb contribution of 0 and 0.541, respectively.[47] The IFD studies depicted that MF due to conformational favorability offers irreversible binding unlike the other ligand and is the best fit (Table 1).

3.7. Anti-acetylcholinestrase Activities of MF and MF-Loaded Chitosan−Collagen Nanocapsules. AChE is a key enzyme in the cholinergic neurotransmission and regulates ACh levels in the brain neurons. Cholinergic dysfunction is associated with the memory, learning, and behavioral symptoms which are evident in the pathogenesis of AD. AChE inhibitors have been found to be one of the most promising therapeutic for AD. These inhibitors inhibit the hydrolysis of AChE at the synaptic cleft, thereby improving the cognitive deficit in AD patients. In the current study, we have evaluated the acetylcholinesterase property of MF and MF-CCNc. The results showed that the AChE activity of MF-CCNc (10−50 μg/mL) achieved a significant inhibition ($p < 0.05$) value of 85.20 ± 1.01% (IC_{50} value < 10 μg/mL), as represented in Figure 8. *In vitro* AChE inhibition assay has shown that both MF and MF-CCNc are active against AChE, and MF showed slightly less activity in comparison to standard drug, that is, donepezil, which is partially due to the solvent interactions of the −OH groups in MF. However, MF-CCNc showed improved ache inhibition in comparison to the MF.

4. CONCLUSIONS

MF is an aporphine alkaloid and is of tremendous medicinal importance as reported in earlier studies. To further increase the efficacy of MF, MF-CCNc were synthesized, which were of the size of 12 ± 2 nm as depicted from their TEM and DLS data. DLS data further revealed that the synthesized nano-

https://doi.org/10.1021/acsomega.1c04459
ACS Omega 2022, 7, 6472−6480

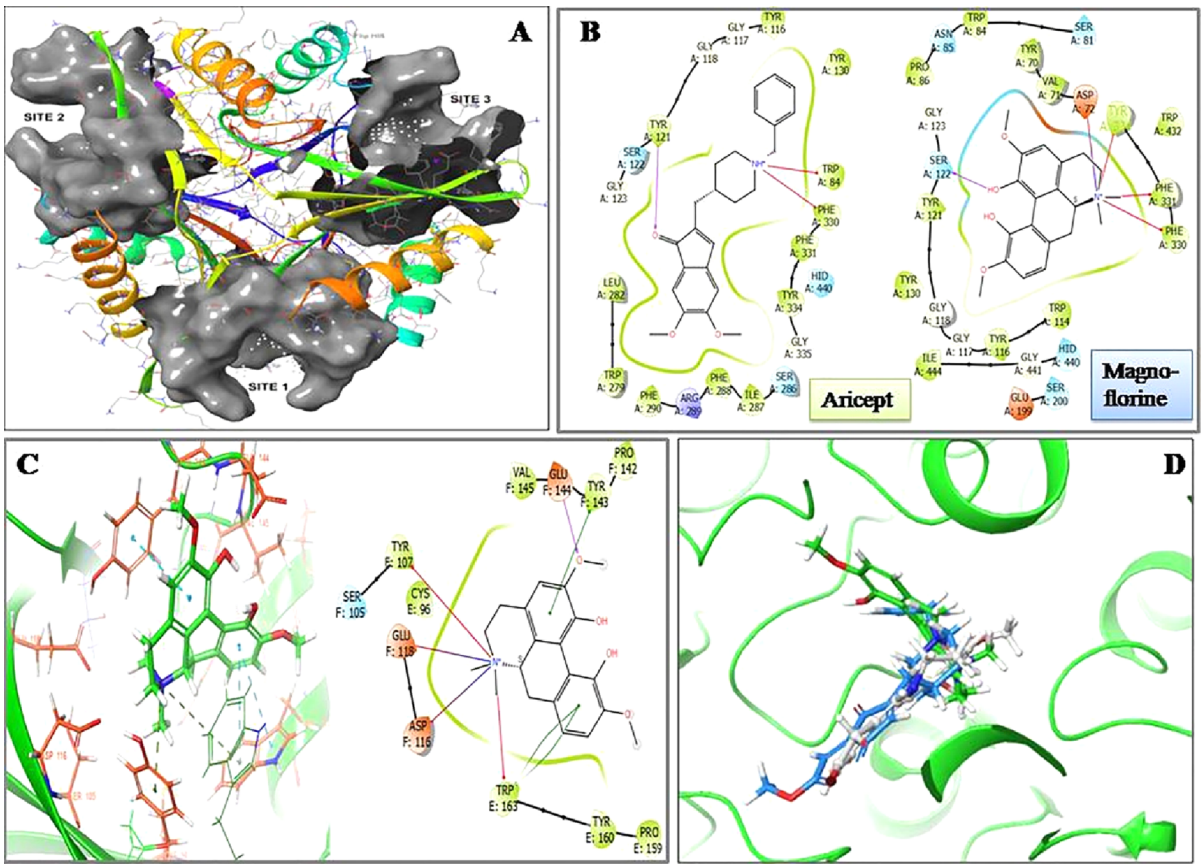

Figure 7. (A) Three similar sites in the trimeric protein. (B) 2D representation of the interaction of the standard and MF ligands with the protein at site 1. (C) Interaction of MF at site I of protein (blue: standard ligand and green: MF). (D) Position and interactions of the active principles and standard ligand deep inside the site I of protein.

Table 1. Docking and XPG Scores of MF in Comparison with Standard

Title	docking score	glide ligand efficiency	glide ligand efficiency sa	glide ligand efficiency ln	glide gscore	glide lipo	glide hbond	glide rewards	glide evdw
Standard	**-9.651**	-0.345	-1.047	-2.228	-9.656	-3.776	-0.353	-3.089	-16.067
Magnoflorine	**-8.209**	-0.328	-0.96	-1.946	-8.64	-2.725	-0.029	-2.808	-11.843

Title	glide ecoul	glide erotb	glide emodel	glide energy	glide einternal	glide eff state penalty	XP GScore
Standard	-14.5	**0.541**	-51.841	-30.56	9.382	0.005	**-4.191**
Magnoflorine	**-16.57**	0	**-49.007**	-28.41	2.455	0.431	**-4.755**

capsules are of good quality with a low PDI of 0.19. Penetration of BBB is the biggest hurdle for the drug development against neurodegenerative diseases; it may be easy for the synthesized nanocapsules mentioned above due to their low size range. The synthesized nanocapsules (MF-CCNc) showed good encapsulation efficiency approximating around 76 ± 1%. Further, the synthesized nanocapsules have shown prolonged release in phosphate buffered saline when compared to the MF. No major cytotoxicity was observed in the case of MF-CCNc at the concentrations, which were used in the experiment. Both MF and the synthesized nanocapsules showed good free radical scavenging properties and can be a good prospect against the oxidative stress, which is seen during the proliferation of neurodegenerative diseases. From the abovementioned results, it can be concluded that the synthesized nanocapsules are of low size range and have good encapsulation efficiency with prolonged release properties and high anti-oxidative properties which may be beneficial for the better delivery of the MF at the site of action for neurodegenerative diseases like Alzheimer's. *In silico* data from the present study revealed that MF have good fitting values for acetylcholinesterase. Induced fit docking studies which were done using donepezil as standard showed higher fitting values

https://doi.org/10.1021/acsomega.1c04459
ACS Omega 2022, 7, 6472−6480

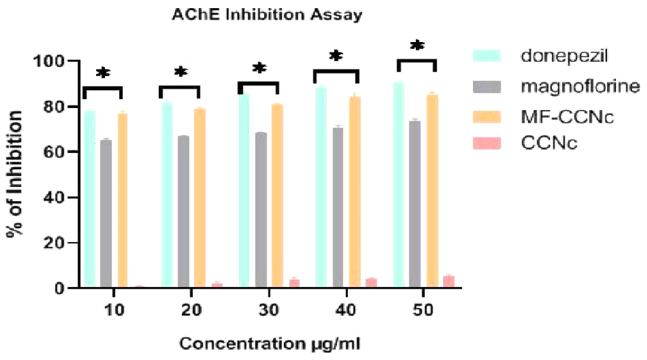

Figure 8. % acetylcholinesterase inhibition of MF and MF-loaded chitosan and collagen nanocapsules and chitosan−collagen nanocapsules. Asterisk (*) over a line denotes the statistically significant ($p < 0.05$) value of control with MF, MF-CCNc, and CCNc. Values are expressed as mean ± SD ($n = 3$).

for MF than that of the standard drug, hence proving the potency of MF for acetylcholinesterase.

AUTHOR INFORMATION

Corresponding Authors

Indu Arora − *Department of Biomedical Sciences, Shaheed Rajguru College of Applied Sciences for Women, Delhi University, New Delhi 110096, India*; Email: aroraindu2004@gmail.com

Mohammed Samim − *Department of Chemistry, School of Chemical and Life Sciences, Jamia Hamdard, New Delhi 110062, India*; orcid.org/0000-0003-1667-8572; Phone: +919891123887; Email: shamim_chem@yahoo.co.in

Authors

Dar Junaid Bashir − *Department of Chemistry, School of Chemical and Life Sciences, Jamia Hamdard, New Delhi 110062, India*

Saliha Manzoor − *Department of Chemistry, School of Chemical and Life Sciences, Jamia Hamdard, New Delhi 110062, India*

Imran A. Khan − *Department of Chemistry, School of Chemical and Life Sciences, Jamia Hamdard, New Delhi 110062, India*

Masarat Bashir − *COTS, Mirgund, SKUAST Kashmir, Srinagar, Jammu and Kashmir 193121, India*

Nidhi Bharal Agarwal − *Centre for Translational and Clinical Research, Jamia Hamdrad, New Delhi 110062, India*

Shweta Rastogi − *Department of Chemistry, Hansraj College, Delhi University, Delhi 110007, India*

Complete contact information is available at: https://pubs.acs.org/10.1021/acsomega.1c04459

Notes

The authors declare no competing financial interest.

ACKNOWLEDGMENTS

D.J.B. is a recipient of Senior Research Fellowship from Indian Council for Medical Research, Government of India [F. no. 45/48/2019-Nan/BMS].

REFERENCES

(1) Chi, H.; Chang, H.-Y.; Sang, T.-K. Neuronal cell death mechanisms in major neurodegenerative diseases. *Int. J. Mol. Sci.* **2018**, *19*, 3082.

(2) Kabanov, A. V.; Gendelman, H. E. Nanomedicine in the diagnosis and therapy of neurodegenerative disorders. *Prog. Polym. Sci.* **2007**, *32*, 1054−1082.

(3) Alzheimer's Association. 2019 Alzheimer's disease, Facts and Figures. *Alzheimer's Dementia* **2019**, *15*, 321−387.

(4) Kumar, A.; Singh, A.; Ekavali. A Review on Alzheimer's disease Pathophysiology and Its Management: An Update. *Pharmacol. Rep.* **2015**, *67*, 195−203.

(5) George-Hyslop, P. H. S.; Petit, A. Molecular biology and genetics of Alzheimer's disease. *C. R. Biol.* **2005**, *328*, 119−130.

(6) Lin, M. T.; Beal, M. F. Mitochondrial dysfunction and oxidative stress in neurodegenerative diseases. *Nature* **2006**, *443*, 787−795.

(7) Hritcu, L.; Ciobica, A.; Artenie, V. Effects of right-unilateral 6-hydroxydopamine infusion-induced memory impairment and oxidative stress, Relevance for Parkinson's disease. *Cent. Eur. J. Biol.* **2008**, *3*, 250−257.

(8) Túnez, I.; Sánchez-López, F.; Agüera, E.; Fernández-Bolaños, R.; Sánchez, F. M.; Tasset-Cuevas, I. Important Role of oxidative stress biomarkers in Huntingtons's disease. *J. Med. Chem.* **2011**, *54*, 5602−5606.

(9) Lilienfeld, S. Galantamine-a novel cholinergic drug with a unique dual mode of action for the treatment of patients with alzheimer's disease. *CNS Drug Rev.* **2006**, *8*, 159−176.

(10) Lane, C. A.; Hardy, J.; Schott, J. M. Alzheimer's disease. *Eur. J. Neurol.* **2018**, *25*, 59−70.

(11) Stowe, R. L.; Ives, N. J.; Clarke, C.; Hilten, J. V.; Ferreira, J.; Hawker, R. J.; Shah, L.; Wheatley, K.; Gray, R. Dopamine agonist therapy in early parkinson's disease. *Cochrane Database Syst. Rev.* **2008**, *16*, CD006564.

(12) Ng, Y. P.; Or, T. C. T.; Ip, N. Y. Plant alkaloids as drug leads for Alzheimer's disease. *Neurol. Int.* **2015**, *89*, 260−270.

(13) Račková, L.; Májeková, M.; Košťálová, D.; Štefek, M. Antiradical and antioxidant activities of alkaloids isolated from Mahonia aquifolium. Structural aspects. *Bioorg. Med. Chem.* **2004**, *12*, 4709−4715.

(14) Hung, T. M.; Lee, J. P.; Min, B. S.; Choi, J. S.; Na, M.; Zhang, X.; Ngoc, T. M.; Lee, I.; Bae, K. Magnoflorine from Coptidis Rhizoma Protects High Density Lipoprotein during Oxidative Stress. *Biol. Pharm. Bull.* **2007**, *30*, 1157−1160.

(15) Kukula-Koch, W.; Kruk-Słomka, M.; Stępnik, K.; Szalak, R.; Biała, G. The evaluation of Pro-cognitive and antiamnestic properties of berberine and Magnoflorine isolated from Barberry species by centrifugal partition chromatography CPC0, in relation to QSAR modeling. *Int. J. Mol. Sci.* **2017**, *18*, 2511.

(16) Jung, H. A.; Min, B.-S.; Yokozawa, T.; Lee, J.-H.; Kim, Y. S.; Choi, J. S. Anti-Alzheimer and Antioxidant Activities of Coptidis Rhizoma Alkaloids. *Biol. Pharm. Bull.* **2009**, *32*, 1433−1438.

(17) Cacciatore, I.; Ciulla, M.; Fornasari, E.; Marinelli, L.; Stefano, A. D. Solid lipid nanoparticles as a drug delivery system for the treatment of neurodegenerative diseases. *Expert Opin. Drug Delivery* **2016**, *13*, 1121−1131.

(18) Saraiva, C.; Praça, C.; Ferreira, R.; Santos, T.; Ferreira, L.; Bernardino, L. Nanoparticle-mediated brain drug delivery: Overcoming blood-brain barrier to treat neurodegenerative diseases. *J. Controlled Release* **2016**, *235*, 34−47.

(19) Li, B.; Han, L.; Cao, B.; Yang, X.; Zhu, X.; Yang, B.; Zhao, H.; Qiao, W. Use of Magnoflorine-Phospholipid complex to permeate blood-brain barrier and treat depression in the CUMS animal model. *Drug Delivery* **2019**, *26*, 566−574.

(20) Zhang, C.; Wan, X.; Zheng, X.; Shao, X.; Liu, Q.; Zhang, Q.; Qian, Y. Dual-functional nanoparticles targeting amyloid plaques in the brains of Alzheimer's disease mice. *Biomaterials* **2014**, *35*, 456−465.

(21) Sánchez-López, E.; Ettcheto, M.; Egea, M. A.; Espina, M.; Cano, A.; Calpena, A. C.; Camins, A.; Carmona, N.; Silva, A. M.;

https://doi.org/10.1021/acsomega.1c04459
ACS Omega 2022, 7, 6472−6480

Souto, E. B.; García, M. L. Memantine loaded PLGA PEGylated nanoparticles for Alzheimer's disease: in vitro and in vivo characterization. *J. Nanobiotechnol.* **2018**, *16*, 32.
(22) Baysal, I.; Ucar, G.; Gultekinoglu, M.; Ulubayram, K.; Yabanoglu-Ciftci, S. Donepezil loaded PLGA-b-PEG nanoparticles: their ability to induce destabilization of amyloid fibrils and to cross blood brain barrier in vitro. *J. Neural Transm.* **2017**, *124*, 33−45.
(23) Bordoni, M.; Scarian, E.; Rey, F.; Gagliardi, S.; Carelli, S.; Pansarasa, O.; Cereda, C. Biomaterials in neurodegenerative disorders: A promising therapeutic approach. *Int. J. Mol. Sci.* **2020**, *21*, 3243.
(24) Lee, L. K. C.; Leong, L. I.; Liu, Y.; Luo, M.; Chan, H. Y. E.; Choi, C. H. J. Preclinical nanomedicines for polyglutamine-based neurodegenerative diseases. *Mol. Pharm.* **2021**, *18*, 610−626.
(25) Fazil, M.; Md, S.; Haque, S.; Kumar, M.; Baboota, S.; Sahni, J. K.; Ali, J. Development and evaluation of rivastagmine loaded Chitosan nanoparticles for brain targeting. *Eur. J. Pharm. Sci.* **2012**, *47*, 6−15.
(26) Rathore, P.; Arora, I.; Rastogi, S.; Akhtar, M.; Singh, S.; Samim, M. Collagen-Curcumin nanocomposites showing an enhanced neuroprotective effect against short term focal cerebral ischemia. *RSC Adv.* **2020**, *10*, 2241.
(27) Ziegler-Borowska, M.; Chelminiak-Dudkiewicz, D.; Siódmiak, T.; Sikora, A.; Wegrzynowska-Drzymalska, K.; Skopinska-Wisniewska, J.; Kaczmarek, H.; Marszałł, M. Chitosan−Collagen Coated Magnetic Nanoparticles for Lipase Immobilization—New Type of "Enzyme Friendly" Polymer Shell Crosslinking with Squaric Acid. *Catalysts* **2017**, *7*, 26.
(28) Chen, M.-M.; Huang, Y.-Q.; Cao, H.; Liu, Y.; Guo, H.; Chen, L. S.; Wang, J.-H.; Zhang, Q.-Q. Collagen/Chitosan film containing biotinylated glycol Chitosan nanoparticles for localized drug delivery. *Colloids Surf., B* **2015**, *128*, 339−346.
(29) Rezaii, M.; Oryan, S.; Javeri, A. Curcumin nanoparticles incorporated collagen-chitosan scaffold promotes cutaneous wound healing through regulation of TGF-β1/Smad7 gene expression. *Mater. Sci. Eng., C* **2019**, *98*, 347−357.
(30) Elnaggar, Y. S. R.; Etman, S. M.; Abdelmonsif, D. A.; Abdallah, O. Y. Intranasal Piperine-Loaded Chitosan Nanoparticles as Brain-Targeted Therapy in Alzheimer's Disease: Optimization, Biological Efficacy, and Potential Toxicity. *J. Pharm. Sci.* **2015**, *104*, 3544−3556.
(31) Elnaggar, Y. S. R.; Massik, M. A. E.; Abdallah, O. Y. Sildenafil citrate nanoemulsion vs. self-nanoemulsifying delivery systems: Rational development and transdermal permeation. *Int. J. Nanotechnol.* **2011**, *8*, 749−763.
(32) Soni, K.; Rizwanullah, M.; Kohli, K. Development and optimization of sulforaphane-loaded nanostructured lipid carriers by the Box-Behnken design for improved oral efficacy against cancer: *In vitro, ex vivo* and *in vivo* assessments. *Artif. Cells, Nanomed., Biotechnol.* **2018**, *46*, 15−31.
(33) Vakilinezhad, M. A.; Tanha, S.; Montaseri, H.; Dinarvand, R.; Azadi, A.; Akbari Javar, H. Application of Response Surface Method for Preparation, Optimization, and Characterization of Nicotinamide Loaded Solid Lipid Nanoparticles. *Adv. Pharm. Bull.* **2018**, *8*, 245−256.
(34) Mathew, A.; Fukuda, T.; Nagaoka, Y.; Hasumura, T.; Morimoto, H.; Yoshida, Y.; Maekawa, T.; Venugopal, K.; Kumar, D. S. Curcumin loaded-PLGA nanoparticles conjugated with Tet-1 peptide for potential use in Alzheimer's disease. *PLoS One* **2012**, *7*, No. e32616.
(35) Amin, F. U.; Shah, S. A.; Badshah, H.; Khan, M.; Kim, M. O. Anthocyanins encapsulated by PLGA@PEG nanoparticles potentially improved its free radical scavenging capabilities via p38/JNK pathway against Aβ1−42-induced oxidative stress. *J. Nanobiotechnol.* **2017**, *15*, 12.
(36) *Schrödinger Suite 2017-3 Protein Preparation Wizard: Epik, Impact, Prime*; Schrödinger, LLC: New York, 2017.
(37) *LigPrep*; Schrödinger, LLC: New York, 2017.
(38) Shanmuganathan, B.; Pandima Devi, K. Evaluation of nutritional profile and antioxidant and anti-cholinesterase activities of padina gymnospora (Phaeophyceae). *Eur. J. Phycol.* **2016**, *51*, 482−490.
(39) Sathya, S.; Shanmuganathan, B.; Saranya, S.; Vaidevi, S.; Ruckmani, K.; Pandima Devi, K. Phytol-loaded PLGA nanoparticle as a modulator of Alzheimer's toxic Aβ peptide aggregation and fibrillation associated with impaired neuronal cell function. *Artif. Cells, Nanomed., Biotechnol.* **2018**, *46*, 1719−1730.
(40) Qi, P.; Zhou, Y.; Wang, D.; He, Z.; Li, Z. A new collagen solution with high concentration and collagen native structure perfectly preserved. *RSC Adv.* **2015**, *5*, 87180−87186.
(41) Queiroz, M. F.; Melo, K. R. T.; Sabry, D. A.; Sassaki, G. L.; Rocha, H. A. O. Does the Use of Chitosan Contribute to Oxalate Kidney Stone Formation? *Mar. Drugs* **2014**, *13*, 141−158.
(42) Rezaii, M.; Oryan, S.; Javeri, A. Curcumin nanoparticles incorporated collagen-chitosan scaffold promotes cutaneous wound healing through regulation of TGF-β1/Smad7 gene expression. *Mater. Sci. Eng., C* **2019**, *98*, 347−357.
(43) Yue, P.-F.; Yuan, H. L.; Yang, M. Preparation, characterization and pharmacokinetic evaluation of puerarin submicron emulsion. *PDA J. Pharm. Sci. Technol.* **2008**, *62*, 32−45.
(44) Baysal, I.; Ucar, G.; Gultekinoglu, M.; Ulubayram, K.; Yabanoglu-Ciftci, S. Donepezil loaded PLGA-b-PEG nanoparticles: their ability to induce destabilization of amyloid fibrils and to cross blood brain barrier in vitro. *J. Neural Transm.* **2017**, *124*, 33−45.
(45) Paul, D. R. Elaborations on the Higuchi model for drug delivery. *Int. J. Pharm.* **2011**, *418*, 13−17.
(46) Jiang, T.; Sun, Q.; Chen, S. Oxidative stress: a major pathogenesis and potential therapeutic target of antioxidative agents in Parkinson's disease and Alzheimer's disease. *Prog. Neurobiol.* **2016**, *147*, 1−19.
(47) Kryger, G.; Silman, I.; Sussman, J. L. Structure of acetylcholinesterase complexed with E2020 (Aricept): implications for design of new anti-Alzheimer drugs. *Structure* **1999**, *7*, 297−307.

https://doi.org/10.1021/acsomega.1c04459
ACS Omega 2022, 7, 6472−6480